Enhanced Proton Loss from Neutral Free Radicals: Towards Carbon-Centered Superacids

*John C. Walton**.

EaStCHEM School of Chemistry, University of St. Andrews, St. Andrews, Fife KY16 9ST, United Kingdom.

Supporting Information

ABSTRACT. Radical centers close to protons are known to enhance their dissociation. Investigation of the generality of this Radical Enhanced Deprotonation (RED-shift) phenomenon and the kinds of structures in which it operates are reported. The pK_as for sulfinic, sulfonic, pentan-2,4-dione and Meldrum's acid species, with adjacent radicals centered on C-, N- and O-atoms, were computed by a DFT method from free energies of deprotonation. All series showed significant RED-shifts that increased with the electronegativity of the radical center. The hugely negative pK_a obtained for a Meldrum's acid with an alkoxyl radical substituent showed it to belong to the superacid class. The ethyne unit was found to be uniquely effective at enhancing acidity and conducting RED-shifts through chains up to and beyond 20 atoms. These connector units enable a radical center to alter the pK_a of a spatially remote acidic group. RED-shifted species were characterized by conjugate radical anions displaying site exchange of spin with electronic charge.

INTRODUCTION

In 1974 Hayon and Simic reviewed what was then known about the acid-base properties of free radicals in solution.[1] One of their conclusions was that the ionization constants of acid radicals were sometimes low in comparison with parent compounds. Twenty years later Radom and co-workers carried out QM computations on the gas phase protonations of carbon-centered organic radicals.[2,3] Continuing this theme they examined the bond dissociation energies and acidities of alcohols and noted that "In general, the CH_3WOH alcohols were found to be less acidic than the related $\bullet CH_2WOH$ radicals" (W represents connector groups).[4] Studer and Curran pin-pointed the enhanced acidity of intermediate cyclohexadienyl radicals as an important driver in base-promoted homolytic aromatic substitution reactions (BHAS).[5] Recent research on the bicarbonate radical [$HOCO_2\bullet$], an important spin-out species of the biological buffer system,[6,7,8,9,10,11] drew attention to its high acidity.[12] The pK_a of this radical is at least 4 log units less than that of carbonic acid [$HOCO_2H$; pK_a = 3.6]; a model in which the unpaired electron (upe) is replaced by an H-atom. Several other radicals, including the biologically important carboxyl [$\bullet C(O)OH$] and hydroperoxyl [$HOO\bullet$] radicals, were also shown to exhibit greatly enhanced acidity in comparison with analogous models. A study of a diverse set of radicals containing carboxylic acid substituents picked out structural features necessary for them to display the phenomenon of Radical Enhancement of Deprotonation.[13] "RED-shift" was adopted as a short and convenient acronym for this phenomenon. Furthermore, ethyne units were shown to be particularly efficient at transmitting the effect through molecular structures.

These discoveries raised questions about the generality of the phenomenon and the extent of the molecular landscape in which it might operate. Could the acidity of other proton donor groups, such as sulfonic, sulfinic and even carbon acids, also be increased by suitably sited and

structured mono-radical substituents? Some very large RED-shifts had been discovered. For example, the pK_a of the hydroperoxyl radical (HOO•, perhydroxyl) at 4.88 compared with a pK_a of 11.75 for model hydrogen peroxide (HOOH) amounted to a RED-shift of more than 6 log units! It was clearly of interest, therefore, to examine the limits achievable for RED-shifts with differing Bronsted acid types. Research with the objective of establishing if deprotonation of sulfonic, sulfinic and carbon acids could be enhanced by neighboring radical substituents is reported in this paper. Furthermore, could radical incorporation push organic acids, unmixed with Lewis acids, towards the superacid class? The investigation was also designed to reveal if the remarkable ability of ethyne spacer units to transmit the effect between carboxylic acid and radical centers would be transferable to other acid types and to probe the reach of such transmission.

COMPUTATIONAL DETAILS

DFT calculations were carried out using the Gaussian 09 suite of programs.[14] The CAM-B3LYP functional[15] with the 6-311+G(2d,p) basis set was employed for most species with the CPCM continuum model[16] with water as solvent. Vibrational frequency calculations were implemented so that GS (no imaginary frequencies) and TS status could be checked (one imaginary frequency) and enthalpies and free energies were adjusted for zero point and thermal corrections to 1 atm and 298 K.

RESULTS AND DISCUSSION

Computation of pK_as

The pK_as of transient radicals are very difficult to measure experimentally because of the high reactivities/short lifetimes of both the neutral acid radicals and their conjugate radical anions. Only a few, usually relying on specialized spectroscopic methods,[17] have been determined and their error limits are necessarily high. A computational method was therefore sought that would output dependable data and would be easy to apply. The literature contains a wide range of computation methods for acid dissociation constants,[18,19] including those of carboxylic acids,[20,21,22,23] and other organic compounds.[24,25,26,27]

$$HA_{aq} \rightarrow H_{aq}^{+} + A_{aq}^{-} \qquad \Delta G_{A\text{-}HA}$$

The pK_a of a Bronsted acid HA is directly proportional to the free energy of deprotonation [$\Delta G_{A\text{-}HA}$] of the acid:

$$\Delta G_{A\text{-}HA} = 2.303RT \times pK_a \qquad (1)$$

Not surprisingly therefore, computational methods focus on various ways of determining free energies of deprotonation. An advantageous approach has been to derive linear correlations of experimental pK_a values, for particular classes of compounds, with DFT computed free energies of deprotonation.[28,29] This method was chosen for the acid radicals of this work and linear regression plots were examined for four classes of model acids having known experimentally determined pK_a values. A previous study of 12 radical reaction types compared results from the high level composite ab initio G4 method,[30] with those obtained with 23 different DFT functionals (plus the MP2 ab-initio method).[12] The CAM-B3LYP functional was found to perform best with radical species and gave lowest mean absolute deviations (MAD). For each set of model acids deprotonation free energies were then computed with this functional making

use of the 6-311+G(2d,p) basis set and with the CPCM continuum model with water as solvent. The experimental free energy of solvation for the proton (-264.2 kcal/mol)[31] was included.

Model organic sulfonic and sulfinic oxy-acids were chosen for study because of their likeness to carboxylic acids. It was deemed that enhanced acidity might also be displayed by other proton donor molecules with suitable radical substituents. Linear regression plots were therefore made of the DFT computed $\Delta G_{A\text{-}HA}$ values with the known experimental pK_as for sets of sulfonic and sulfinic acids, for imides and for carbonyl compounds. The experimental ionization constants were taken from published compilations.[32,33,34] Details of the computations are in the Supporting Information together with a composite graph of plots for each acid type (Figure S1) showing the good consistency of the data. In this way the relationships (2) to (5) were obtained; equation (6) was derived previously by the same method for model carboxylic acids:[13]

Sulfonic acids:	$pK_a^{SO3H} = 1.050\times\Delta G_{A\text{-}HA} + 0.554$	$R^2 = 0.962$	MAD = 0.82	(2)
Sulfinic acids:	$pK_a^{SO2H} = 0.156\times\Delta G_{A\text{-}HA}$	$R^2 = 0.13$	MAD = 0.19	(3)
Imides and amides:	$pK_a^{NH} = 0.366\times\Delta G_{A\text{-}HA}$	$R^2 = 0.975$	MAD = 0.34	(4)
Carbonyls	$pK_a^{CH} = 0.418\times\Delta G_{A\text{-}HA} - 2.272$	$R^2 = 0.961$	MAD = 0.52	(5)
Carboxylic acids	$pK_a^{CO2H} = 0.287\times\Delta G_{A\text{-}HA} + 0.013$	$R^2 = 0.944$	MAD = 0.46	(6)

The lines for the carboxylic acids, imides and amides pass very close to the origin and the line for the sulfonic acids also has a very small intercept (see Figure S1). This behavior is in good accord with the direct proportionality inherent in general equation (1). Available experimental pK_a data for sulfinic acids covered too narrow a range for a satisfactory correlation to be obtained ($R^2 = 0.13$). However, the data matched the general trend observed for the other series, so a zero intercept was assumed and the regression line (3) was obtained. The only regression

line with a significant intercept was that of the carbonyls (5) where compound diversity was somewhat greater. Very acceptable MADs of the computed pK_as from the experimental ones (shown to the right of the relationships) were obtained for the model acids. This data implied that realistic estimates for the pK_as of transient acidic radicals of each class could thereby be obtained.

RED-Shifts in Sulfonic and Sulfinic Acid Radicals

The above-mentioned investigation with carboxylic acids had shown that large RED-shifts usually resulted when the radical center was in close proximity to the acid group. Alkanic (including CH_2), alkenic and aromatic spacer groups between the radical center and the CO_2H group transmitted the effect poorly, if at all, but ethyne and bicyclo[1.1.1]pentanic spacers did conduct RED-shifts. Sets of sulfinic (**1** to **4**) and sulfonic (**5** to **8**) acid radicals with analogous structural features were chosen for study (Scheme 1) together the corresponding models in which the upes were replaced by H-atoms (**1H** to **8H**). The $\Delta G_{A\text{-}HA}$ values for ionizations of the acid radicals and their model acids were computed by the DFT method described above. Then expressions (2) and (3) were employed to obtain the corresponding pK_a values. The data for the acid radicals and the non-radical acid models is compared in Table 1. The magnitude of any RED-shift is expressed by ΔpK_a [defined as pK_a(model) - pK_a(radical)] which amounts to a quantitative yardstick for the phenomenon.

Scheme 1. Sulfonic and Sulfinic Acid Radicals with Corresponding Non-Radical Models

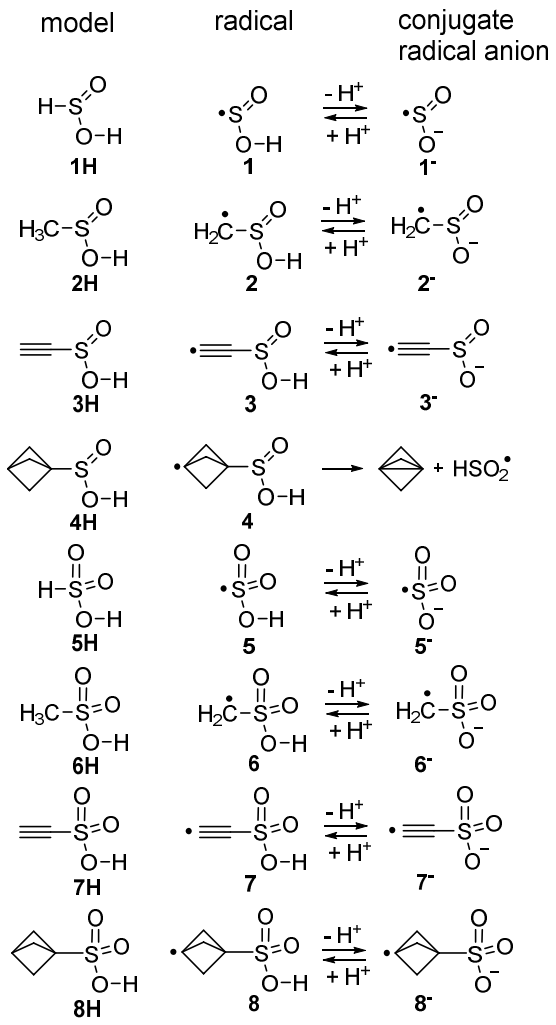

The small or negative pK_a values (Table1, column 3) revealed that, as expected, both sulfinic and sulfonic models and radicals were all strong acids; sulfonic being significantly stronger. Note that the ΔpK_as were all either positive or near zero indicating that the radical center either had no effect or it enhanced acidity. As seems reasonable, no diminishment of acidity was observed for any structural arrangement. A small RED-shift (0.88) was induced in sulfinic radical **1** and a substantial RED-shift of 4.11 units in the ethynesulfinic acid radical **3**. On the other hand, essentially no RED-shift was present in the methylenesulfinic acid radical **2**. This was analogous to the carboxymethyl acid radical $^{\bullet}CH_2–CO_2H$ which also showed no RED-shift.

Bicyclo[1.1.1]pentanesulfinic acid model **4H** was found to be a strong acid comparable to methanesulfinic acid, but the corresponding radical **4** was predicted to be unstable and to spontaneously dissociate to [1.1.1]propellane and the $HSO_2^{\bullet}$ radical.

Table 1. Data for Deprotonations of Sulfinic (**1** to **4**) and Sulfonic (**5** to **8**) Acid Radicals and for Corresponding Models.

Acid dissociation	$\Delta G_{A\text{-}HA}$ kcal/mol	pK_a	ΔpK_a
1H to 1H$^-$	11.15	1.76	
1 to 1$^-$	5.58	0.88	0.88
2H to 2H$^-$	13.17	2.08	
2 to 2$^-$	12.06	1.91	0.17
3H to 3H$^-$	5.26	0.83	
3 to 3$^-$	-20.73	-3.28	4.11
4H to 4H$^-$	13.37	2.12	
5H to 5H$^-$	-5.69	-5.42	
5 to 5$^-$	-8.70	-8.59	3.17
6H to 6H$^-$	-1.19	-0.69	
6 to 6$^-$	-3.29	-2.90	2.21
7H to 7H$^-$	-9.79	-9.72	
7 to 7$^-$	-12.18	-12.23	2.51
8H to 8H$^-$	-1.09	-0.59	
8 to 8$^-$	-3.24	-2.85	2.25

A somewhat different picture emerged from the sulfonic acid data. As expected, moderate RED-shifts were obtained for the sulfonic acid radical itself **5** and for the ethynesulfonic acid radical **7**. Interestingly, the methylene spacer in radical **6** and the bicyclo[1.1.1]pentane spacer in **8** also permitted moderate enhancement of acidity. Previous research had indicated that RED-shifts occurred when the structure made possible site exchange of spin with charge. The significant RED-shift of methylene-sulfonic acid radical $\mathbf{6}^-$ can be attributed the pyramidal SO_3^- group

permitting this; possibly because the *p*-orbital of the $CH_2^{\bullet}$ group necessarily eclipsed one of the S=O bonds. No such eclipsing occurred with the CO_2^- of the non-RED-shifted carboxymethyl radical or the SO_2^- group of methylenesulfinic acid radical (**2**).

Modest RED-Shifts for Imidyl and Related Acid Radicals

Several imides were known to be good proton donors, so the possibility of radical enhancement of proton release from imide N-atoms was next investigated. The azetidine-2,4-dione unit (see **9H**) offers a symmetrical, planar platform permitting comparatively close approach of an upe to the anionic center in the conjugate base $\mathbf{9}^-$ (Scheme 2). The free energies of proton loss from the imidyl radicals **9a-f** and the corresponding model imides were computed as before. Then equation (4) was employed to obtain the corresponding pK_a values. The data (Scheme 2) showed that again all the ΔpK_a were positive or near zero. However, the presence of the upe caused only modest RED-shifts in the parent radical (R = H) or with either electron-repelling (R = *t*-Bu, Me_3Si) or electron-withdrawing substituents (R = F) at the formal radical center. Furthermore, ΔpK_a was close to zero for the Ph and OMe substituents that delocalized spin away from the anionic center.

Similarly, in the 1,3,5-dioxazinane-4,6-dion-4-yl radical **10** only a modest RED-shift was induced at the imide center (Scheme 2). The situation was somewhat similar in the 1,4-dihydropyridin-4-yl radical **11** where only a modest RED-shift was computed. Evidently, neither the C(=O) units of azetidine-2,4-diones $\mathbf{9}^-$, nor the C(=O)O units of $\mathbf{10}^-$ nor the C=N double bonds of $\mathbf{11}^-$ facilitated substantial exchange of charge and/or spin.

Scheme 2. Computed RED-Shifts (ΔpK_a) in Azetidindionyl and Related Imidyl Radicals.

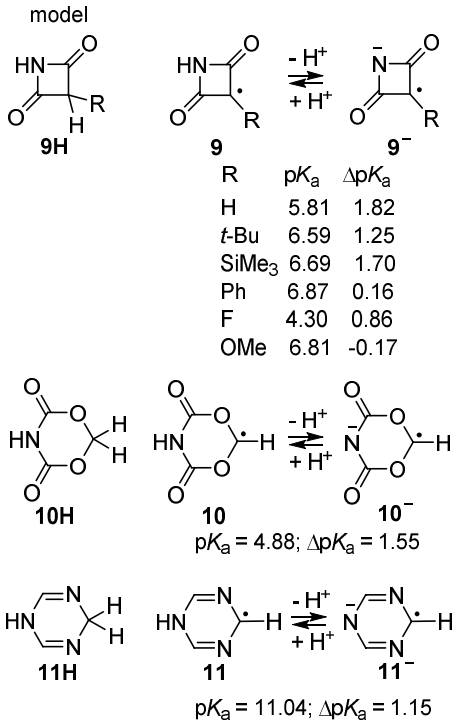

RED-Shifts in Carbon Acids

Generation of carbanions by deprotonation of suitably activated C–H bonds is an extremely important process in numerous organic preparative sequences. Exceptional interest is therefore attached to discovering if the lability of appropriate C–H bonds can be enhanced by neighboring radical centers. 1,3-Dicarbonyl compounds are popular reagents for carbanion (enolate) production, so two types with contrasting acidities were chosen for study. 1,3-Diketones are weak acids with pK_as in the range 9 to 11 whereas Meldrum's acid (2,2-dimethyl-1,3-dioxane-4,6-dione)[35,36] and derivatives are comparatively strong acids with pK_as close to 5 units. Two suites based on these structures and containing radicals centered on different elements are set out in Chart 1, which also lists the pK_as, derived from $\Delta G_{A\text{-}HA}$s by use of expression (5), together with the ΔpK_as relative to the corresponding non-radical models.

Chart 1. Computed pK_as and RED-Shifts (ΔpK_a) in Pentan-2,4-dione and Meldrum's Acid Derivatives.

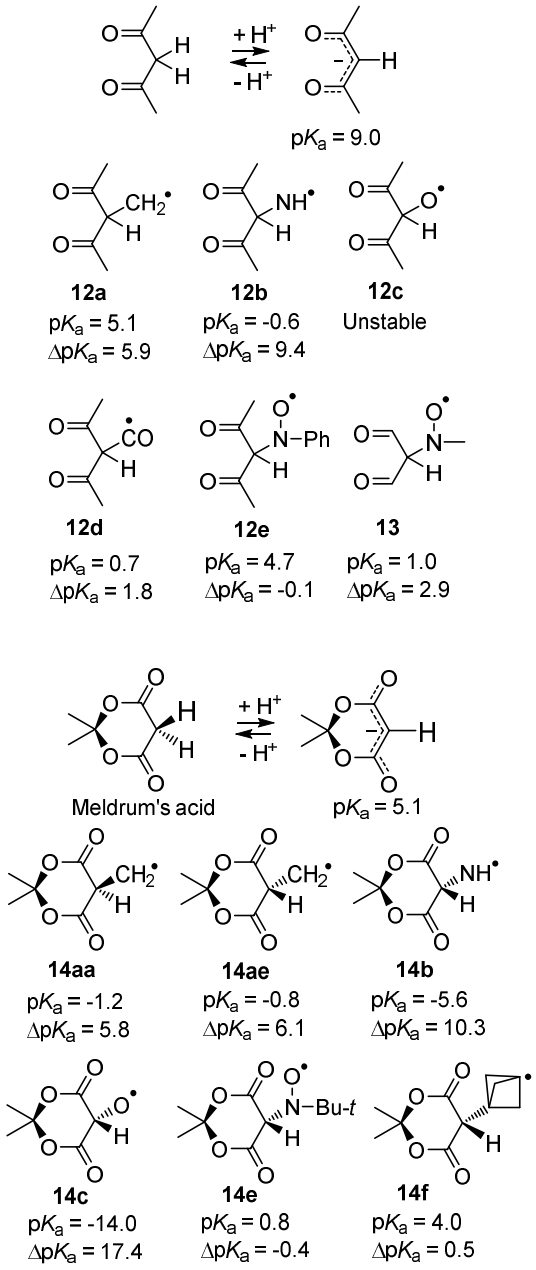

Within the pentan-2,4-dione set, radical **12a** with a $CH_2^{\bullet}$ group adjacent to the leaving proton, showed a substantial RED-shift (5.9 units). The more electronegative aminyl group ($HN^{\bullet}$) in **12b** induced a very large RED-shift of 9.4 log units. The corresponding alkoxyl radical **12c** was

unstable and spontaneously dissociated to the acetyl radical and 2-oxopropanal. By way of contrast, formyl radical **12d** and nitroxide (aminoxyl) radical **12e** displayed small and essentially zero RED-shifts respectively. For these two species charge/spin exchange appeared to be blocked because steric factors prevented effective orbital overlap in the conjugate radical anions. In support of this, a significant ΔpK_a (2.9) was found for nitroxide radical **13** in which smaller substituents permitted internal rotation around the C–N(O•) bond. Of course, the lack of bulky substituents would mean nitroxide **13** would be a transient, rather than a persistent radical.

The 6-member ring of Meldrum's acid adopts a quasi-chair conformation such that a radical substituent may be quasi-axial as in **14aa** or quasi-equatorial as in **14ae**. The computed $\Delta G_{A\text{-}HA}$s, and hence the corresponding pK_as, differed by only small amounts for the two conformations (Chart 1). This molecular structure was found to be particularly well suited to RED-shift generation for certain radical types. For example, even the methylene radical substituent (**14a**) gave rise to a large RED-shift and introduction of the more electronegative aminyl radical (**14b**) led to a huge RED shift of 10.3 units. The pK_a of **14c**, with the even more electronegative oxyl substituent, was a remarkable -14 log units corresponding to the largest recorded RED-shift of 17.4 units! This acidity puts Meldrum's alkoxyl radical **14c** in the same class as superacids such as fluorosulfuric and triflic acid with pK_as of -10 and -13 units respectively. Alkoxyl radical **14c** would be a very short-lived species but, on generation, it could give rise to a huge transient increase in acidity. By way of contrast, the Meldrum's nitroxide **14e** and the Meldrum's bicyclo[1.1.1]pentanyl radical **14f** displayed essentially zero RED-shifts.

Figure 1 compares the distribution of charge (blue numbers), spin density (red numbers) and HOMO amplitudes in the anion of the non-radical model **14aH**$^-$ with the analogous data for conjugate radical anions **14a**$^-$, **14c**$^-$ and **14g**$^-$ of the Meldrum's systems. In model CH_3-

containing anion **14aH**$^{-}$ almost all the negative charge appears in the propan-dione unit and the HOMO also has its highest amplitude associated with this moiety. The increased stabilization of the $CH_2^{\bullet}$-containing radical anion **14a**$^{-}$ is a consequence of the distribution of negative charge away from the propan-dione and onto the CH_2 group, coupled with delocalization of spin density in the other direction away from the CH_2 group and onto the propan-dione unit (Figure 1). This exemplifies the charge/spin site exchange process that is characteristic of RED-shift systems. The HOMO of **14a**$^{-}$ consists of a π-system enveloping both propan-dione and CH_2 groups. The conjugate alkoxyl radical anion **14c**$^{-}$, with the huge 17.4 unit RED-shift, has even more negative charge at the radical center and greater spin density distributed to the propan-dione unit. Radical anion **14g**$^{-}$, containing a formyl radical center, has significant negative charge removed from its propan-dione unit to the formyl group. However, the HOMO is a σ-orbital, out of conjugation with the π-system of the propan-dione unit, so the spin density remains virtually all on the CO group (Figure 1). Consequently, charge/spin exchange is minor and only a small RED-shift results.

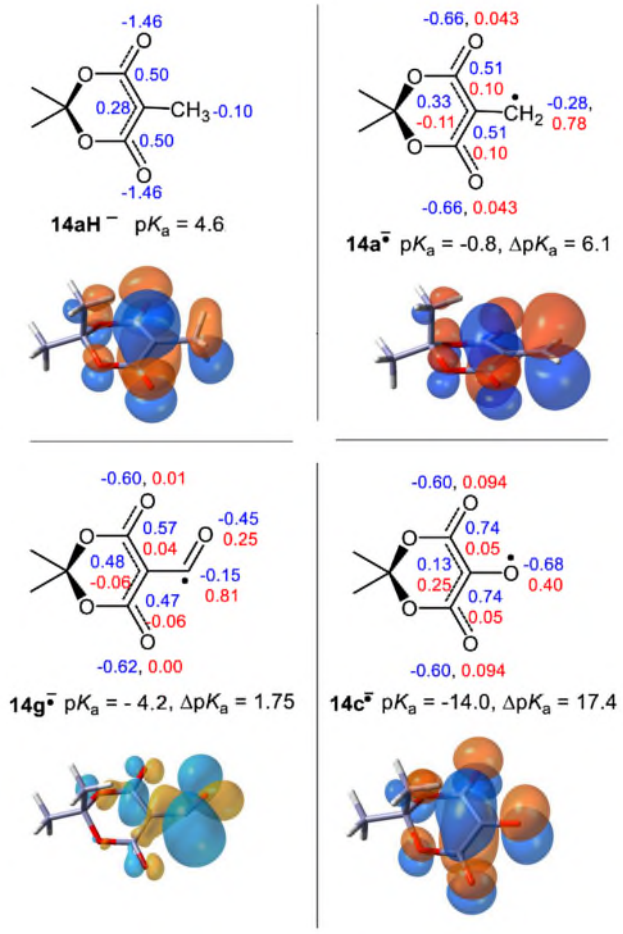

Blue numbers are the electronic charges; red numbers are the spin densities on adjacent atoms.

Figure 1. Charge and Spin Distribution and HOMO Amplitudes of Meldrum's Acid Type Radical Anions.

Influence of Ethyne Radicals and Multiple Ethyne Spacer Units

Ethynesulfinic (**3**) and ethynesulfonic acid radicals (**7**) exhibited substantial RED-shifts (Table 1), as did ethynecarboxylic acid radical. The influence of the ethyne structural unit was intriguing as it appeared to be uniquely effective at enhancing acidity and conducting RED-shifts through chains of atoms. The consequence of introducing it into the two 1,3-dicarbonyl systems was next investigated. RED-shift transmission through polyethyne chains was also examined for

sulfinic acid radicals **15a** to **15g** with up to 6 ethyne units, for sulfonic acid radicals **16a** to **16e** with up to 4 ethyne units, for pentan-2,4-dione radicals **17b** to **17k** with up to 10 ethyne units and for Meldrum's acid derivatives **18b** to **18k** also with up to 10 ethyne units (see Scheme 3).

Scheme 3. Poly-Ethynyl Sulfinic, Sulfonic and Carbon Acid Radicals.

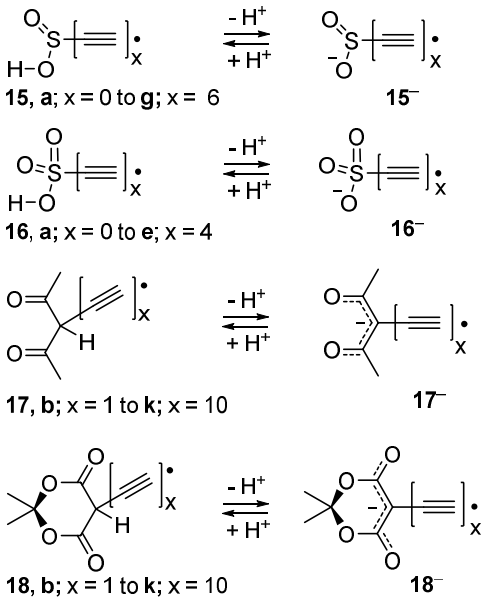

Table 2 contains the pK_a and ΔpK_a computational results for the members of the four poly-ethynyl series, for specified numbers of C-atoms in their chains [C_n].

Table 2. Computed pK_a and ΔpK_a Data for Deprotonations of Poly-Ethynyl Acid Radicals.

C_n / radical	0 a	2 b	4 c	6 d	8 e	10 f	12 g	14 h	16 i	18 j	20 k
16 pK_a	-8.59	-12.23	-16.31	-15.24	-14.31						
ΔpK_a	3.17	2.51	5.77	4.31	3.08						
15 pK_a	0.88	-3.27	-2.49	-1.63	-1.00	-0.55	-0.63				
ΔpK_a	0.88	4.11	3.10	2.16	1.48	1.01	1.07				
17 pK_a		-11.85	-9.21	-8.68	-8.10	-7.68	-7.84	-7.80	-7.36	-7.36	-7.43
ΔpK_a		16.08	11.78	10.41	9.42	8.72	8.95	9.67	9.54	8.15	8.25
18 pK_a		-14.97	-13.88	-11.54	-10.54	-9.91	-9.78	-8.82	-9.45	-9.56	-8.72
ΔpK_a		14.03	11.63	8.62	7.13	6.37	6.21	5.39	5.89	6.12	3.82

Figure 2 compares the pK_as of the four series of poly-ethynyl radicals (open squares) with those of the corresponding (non-radical) model acids (closed circles) as a function of chain length [C_n].

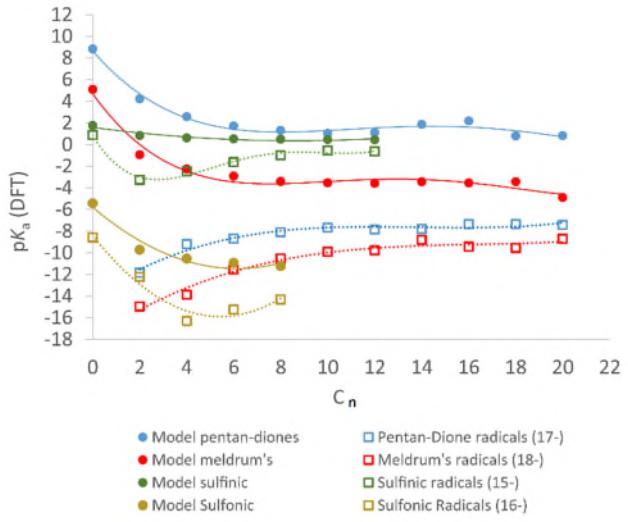

Figure 2. Computed pK_as for Poly-Ethynyl Acid Radicals and Models as a Function of Chain Length.

The pK_as of model acids (filled circles) from *all four sets* are less negative/more positive than those of corresponding radicals (open squares). Hence there are significant RED-shifts for each acid type and for all chain lengths. Initially the model pK_as decreased as C_n increased before leveling off after 6 to 8 atoms (3 to 4 ethyne units). The pK_as of the radicals with sulfonic (**15**$^-$, brown squares), pentan-dione (**17**$^-$, blue squares) and Meldrum's (**18**$^-$, red squares) acids showed they were all extremely strong acids even up to 10 ethyne spacers. The pK_as of the mono-ethynyl-members **15b**, **17b** and **18b** were hugely negative and were on a par with those of the well-known sulfonic superacids (see above). Carbon-based superacids are rare and the ethynyl-dicarbonyl radicals **17b** and **18b** are members, though transient ones, of this uncommon class.[37,38] The acidity of the radicals reduced as the number of spacer alkyne units increased, so

these pK_as tended towards those of the corresponding models, but the incline was shallow such that the approach was remarkably slow (Figure 2). Amazingly the RED-shift remained significant and was transmitted even beyond 10 ethyne units for both the pentan-dione (**17**$^-$) and Meldrum's (**18**$^-$) series. The RED-shifts for the four series are shown in Figure 3 as a function of C_n.

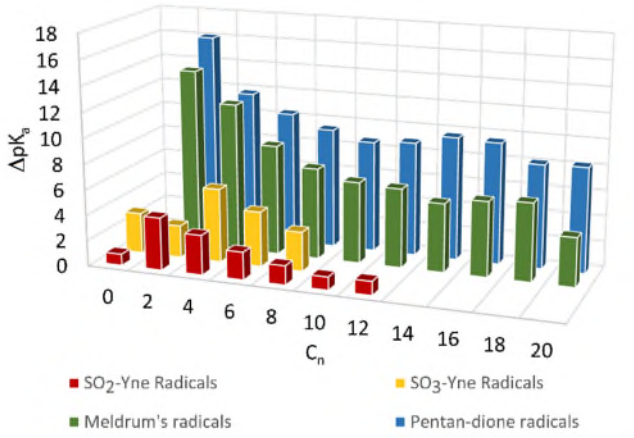

Figure 3. Plots of RED-Shift (ΔpK_a) as a Function of Alkyne Chain Length C_n in Poly-Ethynyl Acid Radicals.

The RED-shifts were largest for the pentan-dione series **17**, were also large for the Meldrum's series **18** but were smaller for the sulfonic series **16** and smallest for the sulfinic set **15**. For all four series, ΔpK_a reduced rapidly as ethyne units were added up to about 4 units. Though increasing the number of ethyne units beyond this led to further decline, this was remarkably slow. It is apparent from Figure 3 that RED-shift is transmitted extremely effectively by the alkyne chains and would be present even beyond 10 ethyne units for the two 1,3-dicarbonyl types.

The key factor in the enhancement of acidity is the thermodynamic stabilization, imparted by the radical centers, to the conjugate radical anions released on deprotonation. Some

insight into this phenomenon can be gained by examining the distribution of spin and electronic charge in these species.

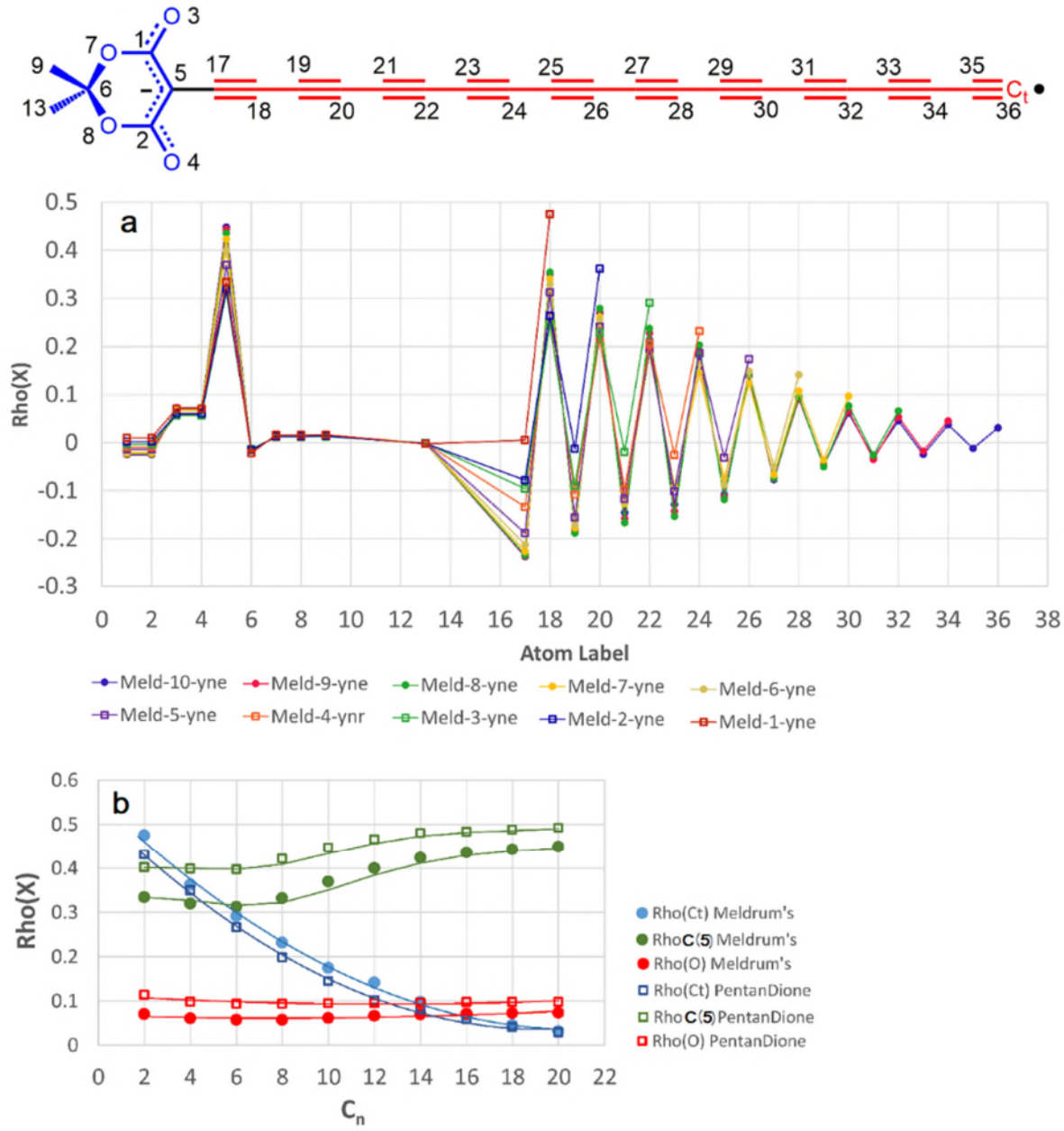

Figure 4. Spin Density Distribution in Poly-Ethynyl Radical Anions. (**a**) Rho(X) at Individual Atoms of All the Radical Anions **18b**$^{-}$ to **18k**$^{-}$; (**b**) Rho(X) at Selected Atoms of Radical Anions **17**$^{-}$ and **18**$^{-}$ as a Function of Alkyne Chain Length C_n.

Although formal structures show the upe at the termini (Ct) of the alkyne chains, Figure 4 shows that in fact, in all the conjugate radical anions **18b**$^{-}$ to **18k**$^{-}$, spin is distributed widely. The left hand region of Figure 4(a), from atom label 1 to 13 refers to the Meldrum's (dimethyl-1,3-dioxane-4,6-dione) part of the structure. Spin density is small in this region, irrespective of the number of ethyne units, except for the central C-5 atom of the pentan-dione unit. At C-5 Rho(C_5) increases as the length of the poly-ethyne chain increases [green circles and squares, Figure 4(b)]. The right hand region of Figure 4(a), from label 17 to 36, refers to the poly-ethynyl chains. The spin density shows an alternating pattern from atom to atom of positive to negative along the chains. The upe is distributed throughout the whole chain for each radical anion such that spin density at the terminal atom (Ct) *decreases* with chain length. Figure 4(b) shows that Rho(Ct) decreased smoothly from around 0.5 for the mono-ethynyl species **18b**$^{-}$ (and **17b**$^{-}$) to about 0.05 for **18k**$^{-}$ as the number of ethyne spacers increased (blue circles and squares). Only a small spin density was associated with the O-atoms of the 1,3-dicarbonyl units [Rho(O)] and this hardly changed as ethyne units were added (red circles and squares, Figure 4b).

Formal structures for the poly-ethynyl radical anions **17**$^{-}$ and **18**$^{-}$ also display the negative charge q(X)/e as contained in the 1,3-dicarbonyl units (Scheme 3). However, Figures 5(a,b) illustrate a more complex situation. Figure 5(a) shows significant negative charge associated with carbonyl O-atoms 3 and 4 and lactone O-atoms 7 and 8; irrespective of the number of ethyne units in the chains. The poly-ethynyl regions show alternating and increasing positive and negative charge for radical anions having up to 5 ethyne units (atom label 26; **18f**$^{-}$) with increasing negative charge at the terminal Ct. However, an abrupt change took place beyond 5 ethynes and, as additional units were added, the alternation was suddenly damped. Net negative charge at Ct was still important even for 10 ethyne spacers. Figure 5b highlights the curious

discontinuity in charge distribution between 5 and 6 ethyne spacers. The computations indicated significant negative charge associated with Ct, even for the mono-ethynyl species **17b**$^{-}$ and **18b**$^{-}$ (Figure 5b, blue squares and circles). The negative charge on Ct increased as up to 5 ethyne units were added in the Meldrum's series (**18**$^{-}$). Lengthening the chain triggered the curious discontinuity to smaller q(Ct); but the trend to increased negative charge was resumed for subsequent additions of ethyne units. That this was not a computational malfunction was supported by the fact that a similar discontinuity was observed in the pentan-dione series (**17**$^{-}$) between 6 and 7 ethyne units (see Figure 5b).

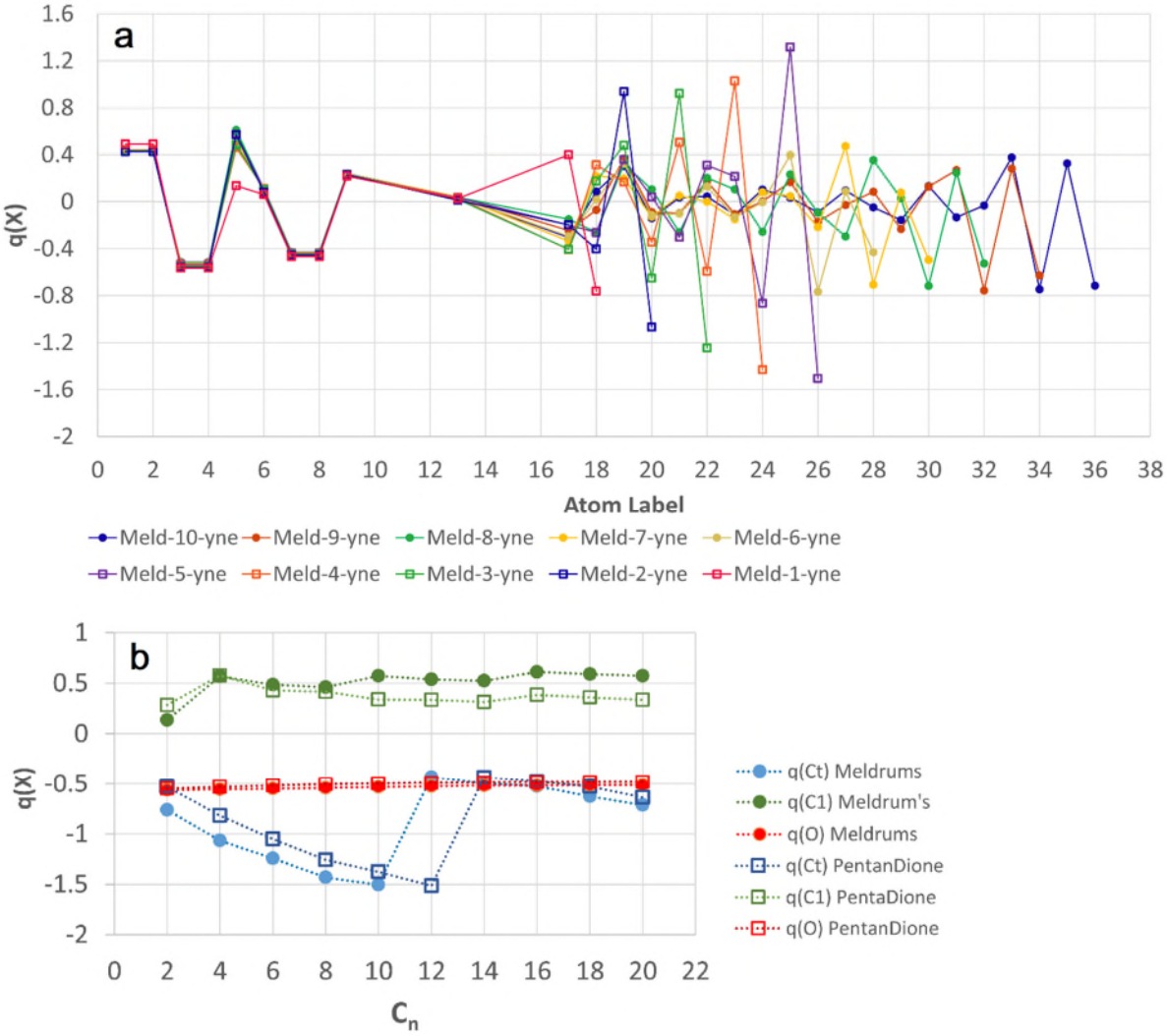

Figure 5. Electronic Charge Distribution in Poly-Ethynyl Radical Anions. (**a**) q(X)/e at Individual Atoms of All the Meldrum's Poly-Ethynyl Radical Anions **18b**$^-$ to **18k**$^-$; (**b**) q(X) at Selected Atoms of Poly-Ethynyl Radical Anions **17**$^-$ and **18**$^-$ as a Function of Alkyne Chain Length C_n.

The computations generated 4 degenerate HOMOs (2 alpha, 2 beta) for every member of the series i.e. **18b**$^-$ to **18k**$^-$ (also for the **17**$^-$ series) together with several additional occupied MOs with energies close to, and getting closer to, those of the HOMOs as the chain lengthened. It seems likely that because of their degeneracy a switch in the orbital(s) associated with the

electronic charge occurred for chains longer than C_{10} (**18f**$^{-}$) with consequent abrupt change in the charge distribution. Negative charge was also associated with the O-atoms of the 1,3-dicarbonyl units (Figure 5b, red circles and squares) and this varied little with chain length. Similarly, the positive charge associated with C1 of the 1,3-dicarbonyl units varied little after an initial increase (Figure 5b, green circles and squares).

The first members of the series **17b** and **18b** had the largest ΔpK_a values and they are characterized by very significant site exchange of spin density and charge. Adding additional ethyne units led to dispersion of both spin density and charge along the poly-ethyne chains which conducted this remarkably efficiently up to and beyond 10 spacer ethynes. Consequently, although the RED-shift diminished, it was still appreciable in 1,3-dione type carbon acids even where the dissociating proton was separated from the formal radical center by 20-atom chains.

Practical Relevance

Radical enhanced acidity could be applied to make possible, or promote, certain chemical and biochemical processes. Some reports of specific chemical and enzymatic instances of this have appeared in the literature. For example, Buckel and co-workers described a dehydratase catalyzed dehydration of (*R*)-2-hydroxyglutaryl-CoA **19** (R = $CH_2CO_2^-$) to (*E*)-glutaconyl-CoA (see Scheme 4).[39] Enzymatic one electron transfer to **19** (R = $CH_2CO_2^-$) yielded ketyl radical anion **20** that eliminated the 2-hydroxy group with formation of carbonyl-stabilized radical **21** (R = $CH_2CO_2^-$, Scheme 4). The γ-H-atom (red) was easily lost because its acidity was enhanced by the adjacent radical center. The resulting allyl radical **22** was then oxidized to afford the glutaconyl-CoA. QM computations indicated a pK_a of about 14 for radical **21**; corresponding to an enhancement of 7.1 units over the pK_a of the corresponding non-radical model.[40] The key

step in an analogous enzyme-catalyzed dehydration of (*R*)-2-hydroxy-4-methylpentanoyl-CoA **19**(R= *i*-propyl) was also identified as deprotonation of intermediate radical **21** (R = *i*-propyl); the allylic radical **22** (R = *i*-propyl) was characterized by EPR spectroscopy.[41] Adaptations of this sequence for functionalization of unactivated γ-H-atoms in ketones, with HO or other leaving groups (L), i.e. molecules with $R_2CHCHLC(=O)R'$ type units, can readily be envisaged.

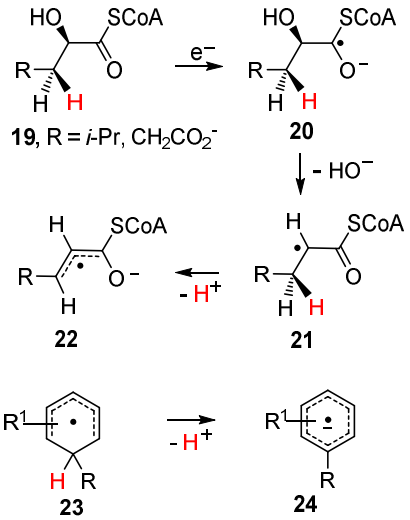

Scheme 4. RED-Shift Facilitation of Chemical and Enzymatic Transformations.

The first step in base-promoted homolytic aromatic substitutions is inter- or intra-molecular addition of a radical ($R^{\bullet}$) to an aromatic or heteroaromatic ring and production of a cyclohexadienyl type radical such as **23**. Re-aromatization may take place by oxidation of **23** to the corresponding cyclohexadienyl cation followed by proton loss. However, the acidity of the proton at C-1 is enhanced by the adjacent radical so it is easily removed by base with production of an aromatic radical anion **24**. The latter may transfer an electron to the radical precursor thus yielding a substituted arene and, with suitable radical precursors, regenerating the initial radical $R^{\bullet}$. Numerous intermolecular and intramolecular examples of these BHAS reactions have been described,[42,43,44] and they can be formulated as electron-catalyzed processes.[5] These examples

widen the scope and generality of the RED-shift phenomenon even further. Opportunities for future applications of these processes in facilitating novel chemical transformations where –CH(R)– activation is required, appear unlimited.

Most of the radicals considered in this study are transient species that could be generated either with steady or pulsed irradiation or by heat. Applications in several types of devices can therefore be foreseen. For example, p*H* could be controlled or varied by applying light or heat with an appropriate radical precursor. Pulses of acidity could be obtained with suitable precursors and equipment. In conjunction with appropriate dyes, light addressed display devices might be achievable. Since a variation in acidity is generally accompanied by variation in conductivity, light operated switching devices appear feasible. The superacid classes of acidic radicals might be applicable as milder and more user friendly reagents than corrosive sulfonic/Lewis superacid mixtures for generating carbo-cations from hydrocarbons.

CONCLUSIONS

In summary, placement of a radical center adjacent to sulfinic, sulfonic or carboxylic acid groups leads in each case to significant enhancement of acidity. The RED-shifts were even more pronounced for the pentan-2,4-dione and Meldrum's acid species. However, only modest deprotonation enhancement occurred for imides of the azetidine-2,4-dione type on introduction of a radical at C-3. In the 1,3-dicarbonyl compound types RED-shifts were obtained with radicals centered on C-, N-, or O-atoms and they increased with the electronegativity of the radical center. The huge radical enhancement in Meldrum's alkoxyl acid **4c** took its acidity into the superacid class. The small or zero RED-shifts for proton donors with formyl or nitroxide radicals can be attributed to their conjugate radical anion structures precluding alignment of orbitals between the radical center and the charge-bearing group.

Bicyclo[1.1.1]pentane and ethyne units were effective as connectors; though ethyne was by far the most efficient. RED-shifts persisted, but progressively diminished, on addition of ethyne spacers up to and beyond 10 such units. The electronic structures of the conjugate radical anions of RED-shifted species were characterized by distribution of spin away from the formal radical center plus distribution of charge away from the formal anionic center(s). The delocalization of charge and spin associated with the RED-shifts implies as a corollary that a remote anion can enhance radical stability.

ASSOCIATED CONTENT

Supporting Information. The Supporting Information is available free of charge on the ACS Publications website at DOI:

Computational methods, deprotonation free energies of model acids, Cartesian coordinates for computed structures (PDF).

AUTHOR INFORMATION

Corresponding Author

*E-mail: jcw@st-andrews.ac.uk. Tel: 44(0)1334 463864.

ORCID

John C. Walton: 0000-0003-2746-6276

Notes

The author declares no competing financial interest.

ACKNOWLEDGMENT

J.C.W. thanks EaStCHEM for financial support.

REFERENCES

(1) Hayon, E.; Simic, M. Acid-Base Properties of Free Radicals in Solution. *Acc. Chem. Res.* **1974**, *7*, 114-121.

(2) Mayer, P. M.; Glukhovtsev, M. N.; Gauld, J. W.; Radom, L. The Effects of Protonation on the Structure, Stability, and Thermochemistry of Carbon-Centered Organic Radicals. *J. Am. Chem. Soc.* **1997**, *119*, 12889−12895.

(3) Mayer, P. M.; Radom, L. Deprotonating Molecules and Free Radicals to Form Carbon-Centered Anions: A G2 Ab Initio Study of Molecular and Free Radical Acidity. *J. Phys. Chem. A,* **1998**, *102*, 4918−4924.

(4) Morris, M.; Chan, B.; Radom, L. Effect of Protonation State and Interposed Connector Groups on Bond Dissociation Enthalpies of Alcohols and Related Systems. *J. Phys. Chem. A,* **2014**, *118*, 2810-2819.

(5) Studer, A.; Curran, D. P. The Electron is a Catalyst. *Nat. Chem.* **2014**, *6*, 765- 773.

(6) Lymar, S. V.; Hurst, J. K. Rapid Reaction Between Peroxonitrite Ion and Carbon Dioxide: Implications for Biological Activity. *J. Am. Chem. Soc.* **1995**, *117*, 8867-8868.

(7) Bonini, M. G.; Radi, R.; Ferrer-Sueta, G.; Ferreira, A. M. D. C.; Augusto, O. Direct EPR Detection of the Carbonate Radical Anion Produced from Peroxynitrite and Carbon Dioxide. *J. Biol. Chem.* **1999**, *274*, 10802-10806.

(8) Hodgson, E. K.; Fridovich, I. Mechanism of the Activity-Dependent Luminescence of Xanthine Oxidase. *Arch. Biochem. Biophys.* **1976**, *172*, 202-205.

(9) Bonini, M. G.; Miyamoto, S.; Di Mascio P.; Augusto, O. Production of the Carbonate Radical Anion during Xanthine Oxidase Turnover in the Presence of Bicarbonate. *J. Biol. Chem.* **2004**, *279*, 51836-51843.

(10) Ramirez, D. C.; Gomez-Mejiba, S. E.; Corbett, J. T.; Deterding, L. J.; Tomer, K. B.; Mason, R. P. Cu,Zn-Superoxide Dismutase-Driven Free Radical Modifications: Copper- and Carbonate Radical Anion-Initiated Protein Radical Chemistry. *Biochem. J.* **2009**, *417*, 341−353.

(11) Liochev, S. I.; Fridovich, I. Mechanism of the Peroxidase Activity of Cu, Zn Superoxide Dismutase. *Free Radical Biol. Med.* **2010**, *48*, 1565−1569.

(12) Bühl, M.; DaBell, P.; Manley, D. W.; McCaughan, R. P.; Walton, J. C. Bicarbonate and Alkyl Carbonate Radicals: Structural Integrity and Reactions with Lipid Components. *J. Am. Chem. Soc.* **2015**, *137*, 16153−16162.

(13) Walton, J. C. Radical-Enhanced Acidity: Why Bicarbonate, Carboxyl, Hydroperoxyl, and Related Radicals Are So Acidic. *J. Phys. Chem. A*, **2017**, *121*, 7761-7767.

(14) Frisch, M. J.; Trucks, G. W.; Schlegel, H. B.; Scuseria, G. E.; Robb, M. A.; Cheeseman, J. R.; Scalmani, G.; Barone, V.; Mennucci, B.; Petersson, G. A.; et al. Gaussian 09, Revision D.01; Gaussian, Inc.: Wallingford, CT, 2013.

(15) Yanai, T.; Tew, D. P.; Handy, N. C. A New Hybrid Exchange-Correlation Functional Using the Coulomb-Attenuating Method (CAM-B3LYP). *Chem. Phys. Lett*. **2004**, *393*, 51-57.

(16) Barone, V.; Cossi, M. Quantum Calculation of Molecular Energies and Energy Gradients in Solution by a Conductor Solvent Model. *J. Phys. Chem. A*, **1998**, *102*, 1995-2001.

(17) Jeevarajan, A. S.; Carmichael, I.; Fessenden, R. W. ESR Measurement of the p*K*a of Carboxyl Radical and Ab Initio Calculation of the Carbon-13 Hyperfine Constant. *J. Phys. Chem.* **1990**, *94*, 1372-1376.

(18) Cheng, J.; Liu, X.; Van de Vondele, J.; Sulpizi, M.; Sprik, M. Redox Potentials and Acidity Constants from Density Functional Theory Based Molecular Dynamics. *Acc. Chem. Res*. **2014**, *47*, 3522-3529.

(19) Zevatskii, Y. E.; Samoilov, D. V. *Russ. J. Org. Chem*. Modern Methods for Estimation of Ionization Constants of Organic Compounds in Solution. **2011**, *47*, 1445-1467.

(20) Schmidt am Busch, M; Knapp, E.-W. Accurate pKa Determination for a Heterogeneous Group of Organic Molecules. *ChemPhysChem* **2004**, *5*, 1513-1522.

(21) Silva, C. O.; da Silva, E. C.; Nascimento, M. A. C. Ab Initio Calculations of Absolute pKa Values in Aqueous Solution. Part 2. Aliphatic Alcohols, Thiols, and Halogenated Carboxylic Acids. *J. Phys. Chem. A,* **2000**, *104*, 2402-2409.

(22) Klicic, J. J.; Freisner, R. A.; Liu, S.-Y.; Guida, W. C. Accurate Prediction of Acidity Constants in Aqueous Solution via Density Functional Theory and Self-Consistent Reaction Field Methods. *J. Phys. Chem. A,* **2002**, *106*, 1327-1335.

(23) Klamt, A.; Eckert, F.; Diedenhofen, M.; Beck, M. E. First Principles Calculations of Aqueous pKa Values for Organic and Inorganic Acids Using COSMO-RS Reveal an Inconsistency in the Slope of the pKa Scale. *J. Phys. Chem. A,* **2003**, *107,* 9380-9386.

(24) Liptak, M. D.; Gross, K. C.; Seybold, P. G.; Feldgus, S.; Shields, G. C. Absolute pKa Determinations for Substituted Phenols. *J. Am. Chem. Soc.* **2002**, *124*, 6421-6427.

(25) Kaminski, G. A. Accurate Prediction of Absolute Acidity Constants in Water with a Polarizable Force Field: Substituted Phenols, Methanol, and Imidazole. *J. Phys. Chem. B,* **2005**, *109,* 5884-5890.

(26) Han, J.; Tao, F-M. Correlations and Predictions of pKa Values of Fluorophenols and Bromophenols Using Hydrogen-Bonded Complexes with Ammonia. *J. Phys. Chem. A,* **2006**, *110*, 257-263.

(27) Eckert, F.; Klamt, A. Accurate Prediction of Basicity in Aqueous Solution with COSMO-RS. *J. Comput. Chem.* **2006**, *27*, 11-19.

(28) See for example: Zhang, S.; Baker, J.; Pulay, P. A. Reliable and Efficient First Principles-Based Method for Predicting pKa Values. 1. Methodology. *J. Phys. Chem. A,* **2010**, *114*, 425-431.

(29) Zhang, S.; Baker, J.; Pulay, P. A. Reliable and Efficient First Principles-Based Method for Predicting pKa Values. 2. Organic Acids. *J. Phys. Chem. A,* **2010**, *114*, 432-442.

(30) Curtiss, L. A.; Redfern, P. C.; Raghavachari, K. Gaussian-4 Theory. *J. Chem. Phys*. **2007**, *126,* 84108-84119.

(31) Tissandier, M. D.; Cowen, K. A.; Feng, W. Y.; Gundlach, E.; Cohen, M. H.; Earhart, A. D.; Coe, J. V.; Tuttle, T. R. The Proton's Absolute Aqueous Enthalpy and Gibbs Free Energy of Solvation from Cluster-Ion Solvation Data. *J. Phys. Chem. A*, **1998**, *102*, 7787-7794.

(32) Serjeant, E. P.; Dempsey, B. *Ionisation Constants of Organic Acids in Aqueous Solution; IUPAC Chemistry Data Series No. 23*; Pergamon Press: Oxford, U.K., 1979.

(33) Kortum, G.; Vogel, W.; Andrussow, K. *Dissociation Constants of Organic Acids in Aqueous Solution*; Butterworths: London, 1961.

(34) Perrin, D. D. *Dissociation Constants of Organic Bases in Aqueous Solution Supplement*; Butterworths: London, 1972; Perrin, D. D. *Dissociation Constants of Organic Bases in Aqueous Solution*; Butterworths: London, 1965.

(35) McNab, H. Meldrum's Acid. *Chem. Soc. Rev.* **1978**, *7*, 345-358.

(36) Dumas, A. M.; Fillion, E. Meldrum's Acids and 5-Alkylidene Meldrum's Acids in Catalytic Carbon-Carbon Bond-Forming Processes. *Acc. Chem. Res*. **2009**, *43*, 440–454.

(37) Reed, C. A.; Kim, K.-C.; Bolskar, R. D.; Mueller, L. Taming Superacids: Stabilization of the Fullerene Cations HC60+ and C60.bul.+. *Science* **2000**, *289*, 101-104.

(38) Juhasz, M.; Hoffmann, S.; Stoyanov, E.; Kim, K.-C.; Reed, C. A. The Strongest Isolable Acid, *Angew. Chem. Int. Ed.* **2004**, *43*, 5352-5355.

(39) Buckel, W.; Keese, R. One-Electron Redox Reactions of CoASH Esters in Anaerobic Bacteria - a Mechanistic Proposal. *Angew. Chem. Int. Ed.* **1995**, *34*, 1502-1506.

(40) Smith, D. M.; Buckel, W.; Zipse, H. Deprotonation of Enoxy Radicals: Theoretical Validation of a 50-Year-Old Mechanistic Proposal. *Angew. Chem. Int. Ed.* **2003**, *42*, 1867-1870.

(41) Kim, J.; Darley, D. J.; Buckel, W.; Pierik, A. J. An Allylic Ketyl Radical Intermediate in Clostridial Amino-Acid Fermentation. *Nat. Chem.* **2008**, *452*, 239-242.

(42) Studer, A.; Curran, D. P. Organocatalysis and C-H Activation Meet Radical- and Electron-Transfer Reactions. *Angew. Chem. Int. Ed*. **2011**, *50*, 5018–5022.

(43) Zhang, B.; Studer, A. Recent Advances in the Synthesis of Nitrogen Heterocycles via Radical Cascade Reactions Using Isonitriles as Radical Acceptors. *Chem. Soc. Rev*. **2015**, *44*, 3505 - 3521.

(44) Budén, M. E.; Bardagí, J. I.; Puiatti, M.; Rossi, R. A. Initiation in Photoredox C–H Functionalization Reactions. Is Dimsyl Anion a Key Ingredient? *J. Org. Chem*. **2017**, *82*, 8325–8333.

Table of Contents Graphic